

Analysis of the Aerodynamic Characteristics of Small-Sized Car Vehicles under the Influence of Steady Crosswind

Lim Wei Chen^{1, a)}, Izuan Amin Ishak^{1, b)}, Mohammad Arafat^{1, c)}, Muhammad Nabil Farhan Kamal¹, Nor Afzanizam Samiran¹ and Ahmad Faiz Mohammad²

Author Affiliations

¹Department of Mechanical Engineering Technology, Faculty of Engineering Technology, Universiti Tun Hussein Onn Malaysia, 84600, Pagoh, Johor, Malaysia.

²Malaysia Japan International Institute of Technology, Universiti Teknologi Malaysia, 54100 Kuala Lumpur, Malaysia

Author Emails

^{b)} Corresponding author: izuan@uthm.edu.my

^{a)} an180285@siswa.uthm.edu.my

^{c)} marafatbd@gmail.com

Submitted: November-December 2022, Revised: January 2023, Accepted: February 21, 2023

Abstract. The crosswind is one of the factors that can lead to a car accident. Crosswind is defined as a side force that causes a vehicle to become unstable and deviate from its desired path. This article focuses on evaluating the flow behaviour and aerodynamic loads that affect vehicle stability when driving in a steady crosswind. In this study, a numerical approach is used with the ANSYS Fluent software as a platform to run the simulation. In this research, the crosswind flow angle (ψ) is varied from 0° to 90° . The incompressible flow surrounding the vehicle is solved using the Reynolds-Averaged Navier-Stokes (RANS) equations in conjunctions with the $k-\epsilon$ turbulence model. The Reynolds number is utilized depending on the velocity of the vehicle which are 2.8×10^6 for high Reynolds number and 7.2×10^5 for low Reynolds number respectively. According to the findings, the crosswind has a significant quantitative and qualitative impact on aerodynamics. In terms of aerodynamic load, the side coefficient (C_s) increases as the crosswind yaw angle increases. When the crosswind yaw angle reaches 60° , there is a significant drop, but it remains almost constant when the crosswind yaw angle reaches 90° . In terms of flow structure, as the crosswind yaw angle increases, the vortex formation on the leeward region expands, increasing the vehicle stability imbalance. Finally, there is no significant difference in the quantitative aerodynamic characteristics of high and low Reynolds numbers.

Keywords: Aerodynamic characteristics, Car vehicle, CFD, Flow structure, Steady Crosswind

INTRODUCTION

Human introduces vehicles is to allow people to get a shield from wind, rain, and dust when people travel in a car. Road vehicles play an important role in society today. Vehicles have many advantages, such as economic and technological advancements, but they also have a negative impact. The most concerning issue reflects the negative impact on the vehicles involved in the accident, which may occur as a result of high demand for transportation and unsafe operation. The transportation demand is concerned with the type of traffic exposure, such as a high volume of traffic and traffic overcrowding. The unsafe operation, on the other hand, is concerned with highly risky vehicle operations, such as the driver, vehicle condition, road, and environmental factors [1], [2]. Strong wind is one of the environmental factors that has raised concerns about the safety of road vehicles [1], [3], [4].

A headwind, crosswind, or tailwind occurs when the natural wind is combined with the direction of travel. Headwinds and tailwinds effect longitudinal vehicle speed primarily by pushing back or forward; they do not create a substantial safety risk [1]. Furthermore, there are two types of crosswind effects on vehicle performance: crosswind aerodynamic and crosswind stability. The crosswind aerodynamics emphasized the significance of time-related changes in the aerodynamic forces operating on vehicles, whereas the crosswind aerodynamics solely focused on the influence of the crosswind on the aerodynamic forces and flow field surrounding the vehicle [4]. Surprisingly, the dominance of the aerodynamics force on vehicle performance is largely ignored. The crosswind

stability focus is on the vehicle motion and dynamic response under the influence of the crosswind. This impact became more significant on the vehicle, which has a large flat surface and a high center of gravity (COG) [1].

Several studies on the effects of crosswinds on heavy ground vehicles have been carried out [5]–[8]. The heavy grounded vehicles such as trains, trucks, and buses since their vast lateral surfaces render them particularly vulnerable to the impacts of crosswind gusts [9]–[11]. Moreover, crosswinds can be especially damaging to heavy trucks. As a result, the improvement in the automotive aerodynamics characteristic alters the researcher's attentiveness to studying the influence of crosswinds not only on heavy vehicles but also on light vehicles such as passenger cars [5].

When driving a small car on the road, external crosswinds have an impact on the driver's ability to control the vehicle. Crosswind conditions are, in general, always present on open roads, and their impact on driving stability increases as vehicle speed increases [12]. The side force and the yaw moment are two aerodynamic parameters that are commonly used to characterize a vehicle's crosswind characteristics. The faster acceleration of vehicle systems has resulted in high energy losses and a decrease in vehicle performance. Therefore, it is necessary to investigate the crosswind stability of a small-sized car in order to evaluate its aerodynamic characteristics by analyzing flow around vehicles and aerodynamic loads. Aerodynamic loads and flow structures around the vehicle are commonly studied in a wind tunnel. Because wind tunnel facilities are rare, much research has focused on modelling aerodynamic loads during crosswind conditions using computational fluid dynamics (CFD) simulations. As a result, the CFD technique was also used in the current study.

This article is organized as follows: an introduction, a material and method section that explains the CFD setup and simulation details, then section 3 describes the results and discussion, and a conclusion at the end.

MATERIALS AND METHODS

Before running the simulation, the first step in performing the CFD analysis is to create a 3D model. The type of simplified vehicle model utilized in this is an A-segment vehicle. Figure 1 shows the detailed geometry and the dimension of this car. The vehicle model of A-segment car is imported and modified in SOLIDWORKS, before being transferred to ANSYS Design Modeler. Due to modelling methodology constraints, such as avoiding the influence of rotational motion and tire wake, the tires and exterior parts are ignored. The computational domain, also known as the enclosure, is defined as the simulation of airflow in a confined area. This is to confirm the flow simulation that will occur inside the enclosure boundary. The fundamental parameters for the validation case on the distances of the length between the inlet and the vehicle, the outlet, and the vehicle are based on the most recent studies [13]–[15]. Before beginning the meshing process, the enclosure must be effective enough to ensure that the computational domain is the optimal size.

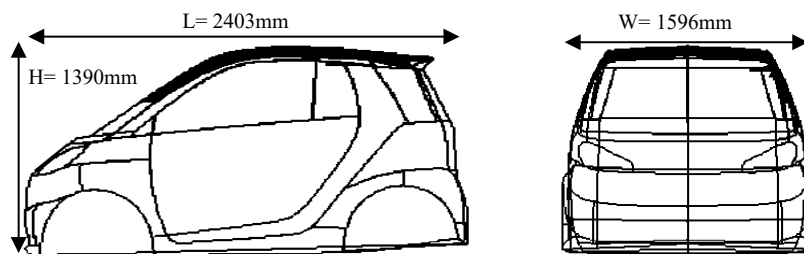


FIGURE 1. Dimensions of the small-sized car used in the current study

The vehicle boundary conditions, including velocity inlet, pressure outlet, vehicle surface, ground, and roof, as well as the computational domain, are exhibited in Figure 2. The boundary conditions are applied for the no crosswind and crosswind conditions. For the current study, a total of 7 yaw angles conditions are considered. The wind speed was 8 ms^{-1} with vehicle speed being 30 ms^{-1} . Additionally, the stationary wall boundary condition was chosen for the ground. After configuring the boundary conditions, turbulence model, initialization, and number of iterations, the simulation process can begin, collecting all necessary data and performing data analysis. The Reynolds number that applies in this study were 2.8×10^6 and 7.2×10^5 which represents the high and low Reynolds number respectively [16]. Aside from that, the current study used the Reynolds-Averaged Navier-Stokes (RANS) with the $k-\epsilon$ turbulence model as it is a computationally efficient technique for CFD analysis.

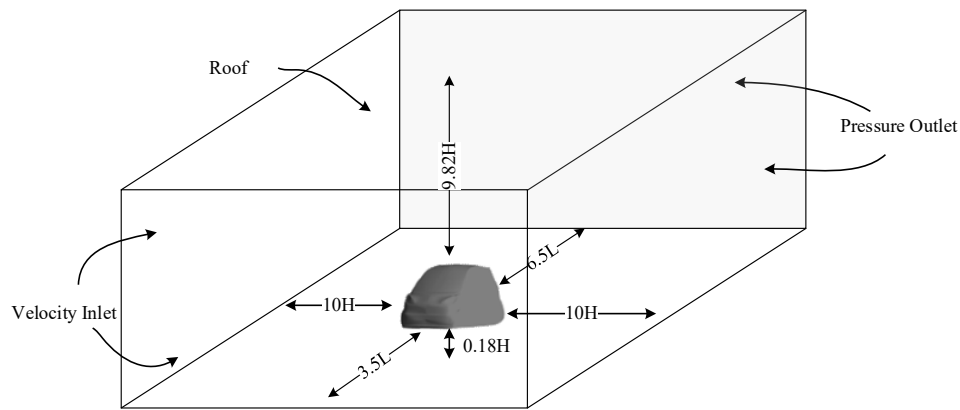


FIGURE 2. Boundary conditions for the numerical analysis

Both numerical simulation and mesh are generated by the Commercial Ansys Fluent Software. One of the most critical and important steps in any type of CFD analysis is generating appropriate meshes and achieving grid independence [17], [18]. As a result, a grid independence test was conducted for the current study utilizing a grid convergence study. Six different curvature variations normal angles with varying mesh resolutions were considered for this purpose. Table 1 displays the meshing parameters and drag coefficient values for six different cases.

TABLE 1. The different meshing and curvature normal angles with drag coefficient value

Case	1	2	3	4	5	6
Curvature normal angles (°)	18	15	12	9	6	3
Number of Nodes	57,137	61,486	67,407	75,118	86,134	105,031
Drag Coefficient (C_d)	0.30	0.29	0.29	0.29	0.29	0.29

According to the simulation data, the drag coefficient value (C_d) for the A-segment car was 0.29. Figure 3 depicts a graph of the drag coefficient considering the number of nodes. The graph shows that the value of the drag coefficient did not improve after the second case. This means that the drag coefficient achieves convergence at 61,486 nodes. As a result, the number of nodes 61,486 was chosen based on the grid-independent test results to carry out the real case simulation. Figure 4 depicts the selected mesh results from the grid independence test.

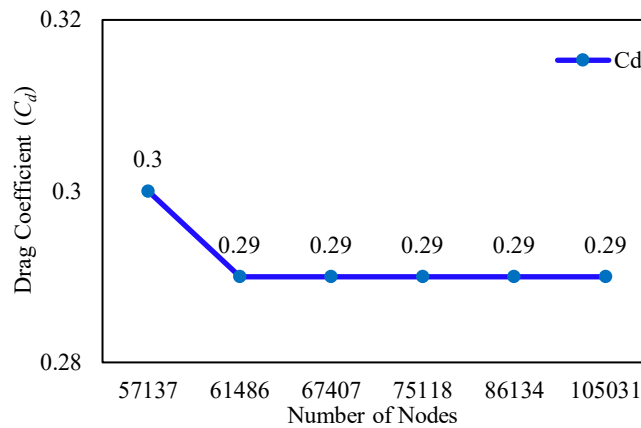


FIGURE 3. Graph of drag coefficient (C_d) against different mesh resolutions

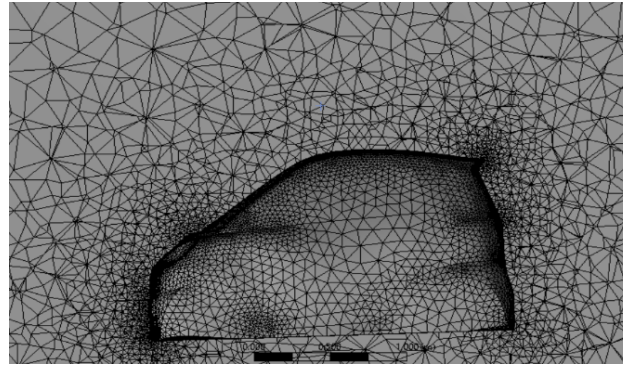


FIGURE 4. Mesh resolution chosen based on grid convergence study

RESULTS AND DISCUSSION

Aerodynamics Loads of the Vehicle

The results of the numerical analysis of the vehicle's aerodynamic loads are presented in this section. Figure 5(a) depicts the drag coefficient versus different crosswind conditions for two different Reynolds numbers. Based on the observations, both Reynolds numbers produce similar results, with the exception of the high yaw angles. Furthermore, for a high crosswind condition, the drag coefficient has a low value. At $\Psi = 30^\circ$, the drag coefficient for the high Reynolds number and low Reynolds number is the peak value. Unfortunately, the trend of the drag coefficient decreases drastically from 30° to 60° yaw angle. Lastly, the trend of the drag coefficient (C_d) had dropped to the lowest at 90° yaw angle.

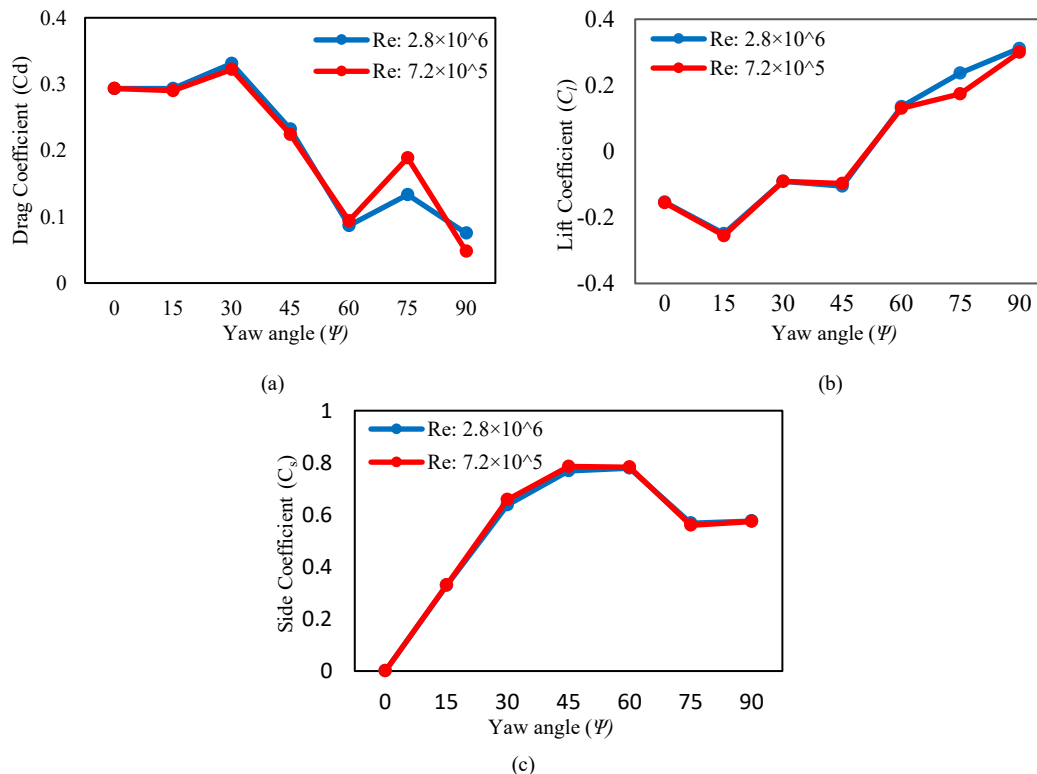


FIGURE 5. Graph of different aerodynamics loads against different crosswind conditions (a) Drag coefficient (b) Lift coefficient (c) Side coefficient

Figure 5(b) depicts the graph behaviour of the lift coefficient in the presence of various crosswind conditions. In general, both high and low Reynolds numbers behaved similarly as the crosswind yaw angle increased, reaching a

maximum at 90° yaw angle. When the crosswind angle is less than 45°, the lift coefficient is negative, whereas it is positive when the crosswind angle is greater than 45°. The negative and positive values of the lift coefficient indicated that the resulting pressure was pointing downwards and upwards, respectively. As a result, the entire body of the vehicle model has a role and significant impact in defining the magnitude of lift coefficient in this range of crosswind yaw angles.

The side coefficient is one of the factors that cause the vehicle to deviate from its direction of travel. Figure 5(c) demonstrated that the difference in Reynolds numbers does not affect the side coefficient value. The maximum point of the side coefficient (C_s) for the high Reynolds number at 60° and the low Reynolds number at 45° yaw angle are 0.779 and 0.786, respectively. Furthermore, the initial point of the side coefficient is zero because the flow is symmetrical to the vehicle body. Lastly, the side coefficient (C_s) exhibits a modest inclining trend when the crosswind conditions increase from 60° to 90° yaw angle.

Flow Structure around the Vehicle

Without Crosswind Condition

The pressure contour with velocity streamlines without crosswind conditions is presented in Figure 6. It is observed that high pressure is located on the vehicle's frontal surface. On the other hand, the low pressure is projected on the front edge of the windward and leeward area. In addition, the low pressure occurs at the roof top of the vehicle which can be seen in Figure 6(b). In terms of the velocity streamline, the streamline begins to divide at the frontal surface of the vehicle, which is also known as the stagnation point. The size of the vortices on both sides is equally symmetrical, which clarifies why the side force is zero at this wind condition. In addition, due to flow separation at both sides of the rear edges, two recirculating vortex bubbles are formed at the rear part of the vehicle.

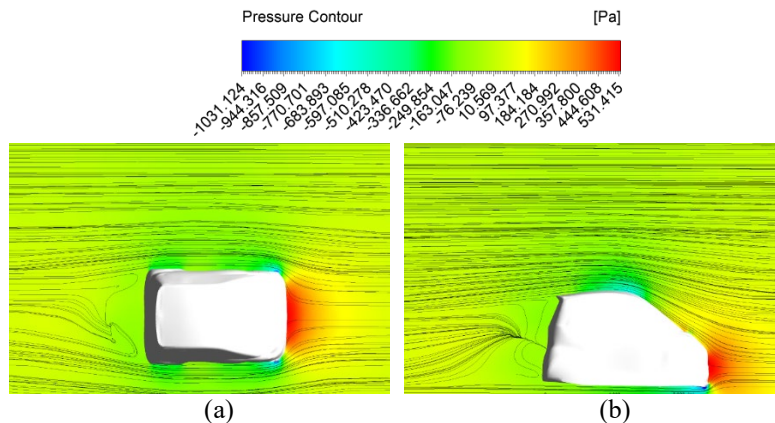


FIGURE 6. Top view and side view of pressure contour superimposed with velocity streamline without crosswind conditions

With Crosswind Condition

Figure 7 depicts a pressure contour with velocity streamlines in a crosswind condition. At 15° crosswind condition, the high-pressure contour had shifted a little right at the frontal surface area of the vehicle compared to 0° yaw angle. In addition, the low pressure is projected at the front edge of the leeward area. The vortex bubbles formed as a result of flow separation of the streamlines. The flow separation will occur at the front edge of the leeward area and both rear edges of the vehicle. As shown in Figure 5, the side coefficient begins to rise in value. The pressure difference between the leeward and windward zones causes this unbalanced flow scenario. The high-pressure region that impacted the vehicle's frontal area gradually migrated to the windward side as yaw angles increased from 15° to 90°. In terms of aerodynamic load, however

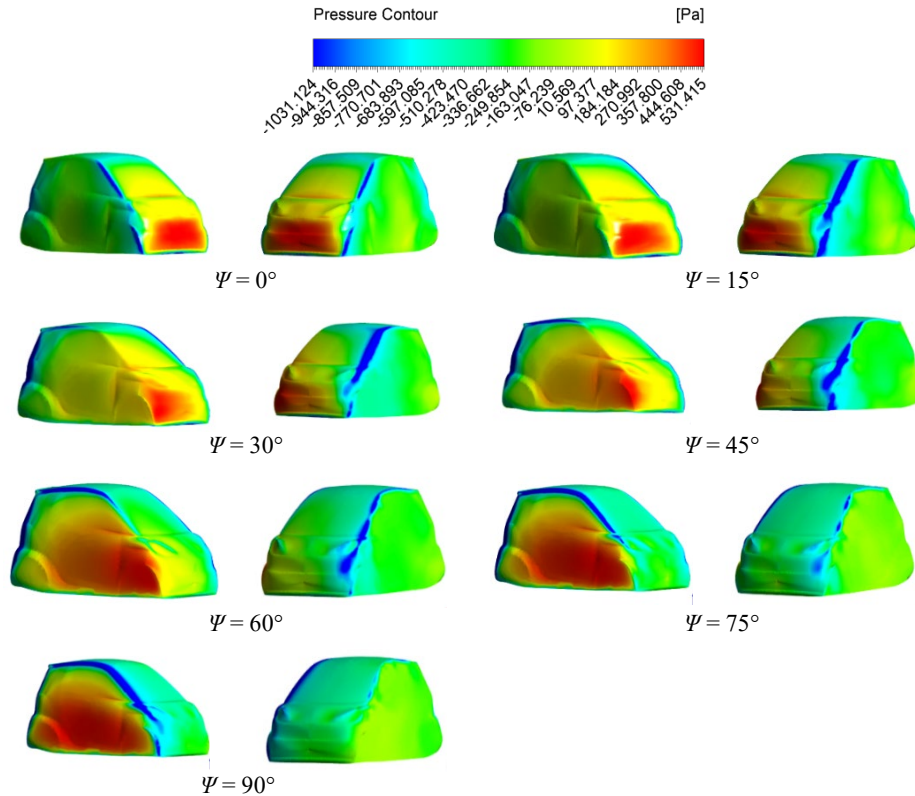


FIGURE 8. Pressure distribution on vehicle surface for different crosswind conditions

CONCLUSION

The current study investigated the aerodynamic characteristics of a small-sized car in a steady crosswind using CFD analysis. When it comes to crosswinds, all aerodynamic factors, including qualitative and quantitative analyses, have a significant impact on the vehicle's dynamic behaviour.

In terms of drag coefficient (C_d), it can be concluded that there is a significant or critical drop in the range at crosswind yaw angles ranging from 30° to 60° . This is because as the crosswind yaw angle increases, so does the drag force that affects the vehicle's frontal surface. Furthermore, the lift coefficient (C_l) is increasing as a result of the crosswind hitting the vehicle model, causing it to slowly migrate to the windward side. As this occurs, the vehicle's overturning becomes more favourable. The side coefficient (C_s) indicates that there is a slight decrease in the 75° yaw angle. Subsequently, comparing the behaviour of low and high Reynold numbers reveals that there is little variation in aerodynamic load qualities.

ACKNOWLEDGMENTS

This research is financially supported by Universiti Tun Hussein Onn Malaysia under UTHM GPPS Grant (H725). The author would also like to thank the Faculty of Engineering Technology, Universiti Tun Hussein Onn Malaysia for providing feasible research facilities for this study.

REFERENCES

1. Z. M. Jawi, R. Sarani, W. S. Voon, A. Farhan, and M. Sadullah, *Weather as a Road Safety Hazard in Malaysia - An Overview* (Malaysian Institute of Road Safety Research (MIROS), Selangor 2009).
2. M. Nabil *et al.*, "A Review of Aerodynamics Influence on Various Car Model Geometry through CFD Techniques," *J. Adv. Res. Fluid Mech. Therm. Sci.*, **88** 109–125 (2021).
3. S. A. Coleman and C. J. Baker, "An experimental study of the aerodynamic behaviour of high sided lorries in cross winds," *J. Wind Eng. Ind. Aerodyn.* **53**, 401–429 (1994).

4. Q. Zhang, C. Su, and Y. Wang, "Numerical investigation on aerodynamic performance and stability of a sedan under wind-bridge-tunnel road condition," *Alexandria Eng. J.* **59**, 3963–3980 (2020).
5. T. Tunay, E. Firat, and B. Sahin, "Experimental investigation of the flow around a simplified ground vehicle under effects of the steady crosswind," *Int. J. Heat Fluid Flow* **71**, 137–152 (2018).
6. L. Carbonne, N. Winkler, and G. Efraimsson, "Use of Full Coupling of Aerodynamics and Vehicle Dynamics for Numerical Simulation of the Crosswind Stability of Ground Vehicles," *SAE Int. J. Commer. Veh.* **9**, 359–370 (2016).
7. C. Proppe and C. Wetzel, "A probabilistic approach for assessing the crosswind stability of ground vehicles," *Veh. Syst. Dyn.* **48**, 411–428 (2010).
8. M. Arafat and I. A. Ishak, "CFD Analysis of the Flow around Simplified Next-Generation Train Subjected to Crosswinds at Low Yaw Angles," *CFD Lett.* **14**, 129–139 (2022).
9. D. McArthur, D. Burton, M. Thompson, and J. Sheridan, "An experimental characterisation of the wake of a detailed heavy vehicle in cross-wind," *J. Wind Eng. Ind. Aerodyn.* **175**, 364–375 (2018).
10. I. A. Ishak, M. S. Mat Ali, M. F. Mohd Yakub, and S. A. Z. Shaikh Salim, "Effect of crosswinds on aerodynamic characteristics around a generic train model," *Int. J. Rail Transp.* **7**, 23–54, (2019).
11. Izuan Amin Ishak *et al.*, "Numerical Analysis on the Crosswind Influence Around a Generic Train Moving on Different Bridge Configurations," *J. Adv. Res. Fluid Mech. Therm. Sci.* **89**, 76–98, (2021).
12. A. Brandt, B. Jacobson, and S. Sebben, "High speed driving stability of road vehicles under crosswinds: an aerodynamic and vehicle dynamic parametric sensitivity analysis," *Veh. Syst. Dyn.*, **60** (2022).
13. T. Favre, "Aerodynamics simulations of ground vehicles in unsteady crosswind." PhD diss., KTH Royal Institute of Technology, 2011.
14. Q.-L. Wang, Z. Wu, X.-L. Zhu, L.-L. Liu, and Y.-C. Zhang, "Analysis of Aerodynamic Performance of Tesla Model S by CFD," in *Proceedings of the 3rd Annual International Conference on Electronics, Electrical Engineering and Information Science*, (Atlantis Press, Paris, 2017) pp. 16–21.
15. Z. M. Saleh and A. H. Ali, "Numerical Investigation of Drag Reduction Techniques in a Car Model," *IOP Conf. Ser. Mater. Sci. Eng.* **671**, 012160, (2020).
16. A. Bornioli, I. Bray, P. Pilkington, and J. Parkin, "Effects of city-wide 20 mph (30km/hour) speed limits on road injuries in Bristol, UK," *Inj. Prev.* **26**, 85–88, (2020).
17. M. Arafat, I. A. Ishak, and A. F. Mohammad, "Influence of mesh refinement on the accuracy of numerical results for Next-Generation High Speed Train," Muar, Unpublished, (2022).
18. M. H. M. William, Youhanna E. and W. A. Oraby., "Investigation of Crosswind Aerodynamics for Road Vehicles Using CFD Technique," in *Eleventh International Conference of Fluid Dynamics*, (ICFD, Alexandria, 2013), pp. 1–11.